Available online at www.sciencedirect.com
ScienceDirect
Ceramics International 37 (2011) 1039–1046
CERAMICS INTERNATIONAL
www.elsevier.com/locate/ceramint

Effect of sphalerite to wurtzite crystallographic transformation on microstructure, optical and mechanical properties of zinc sulphide ceramics

P. Ramavath [a], P. Biswas [a], R.S. Kumar [a], V. Mahendar [a], G.V.N. Rao [a], U.S. Hareesh [a], R. Johnson [a,*], N.E. Prasad [b]

[a] International Advanced Research Centre for Powder Metallurgy and New Materials, PO Balapur, Hyderabad 500005, India
[b] Regional Centre for Military Airworthiness (Materials), CEMILAC, DRDO, PO Kanchanbagh, Hyderabad 500058, India

Received 15 July 2010; received in revised form 11 October 2010; accepted 13 November 2010
Available online 28 December 2010

Abstract

Zinc sulphide (ZnS) ceramics synthesized by chemical vapour deposition (CVD) were subjected to post CVD thermal treatments at 850 and 1050 °C in inert atmosphere under pressureless conditions. The samples were found to undergo cubic (sphalerite) to hexagonal (wurtzite) crystallographic transformation at around 1020 °C as confirmed by dilatometric and X-ray diffraction studies. The paper reports the effect of transformation in terms of structure – both crystallography and microstructure. Further, the effects of this transformation on the optical and mechanical properties are also analyzed. The increase in grain size was found to be beneficial for the IR transmission of sphalerite (cubic) phase while, the presence of wurtzite (hexagonal) was found to reduce the transmission significantly. A detailed evaluation of the nature and characteristics of the fracture revealed that the ZnS ceramics failed predominantly by low energy, quasi – cleavage fracture. It was also confirmed that the mechanical properties of this material vary with the extent (area fraction) of quasi – cleavage facets.
© 2011 Elsevier Ltd and Techna Group S.r.l. All rights reserved.

Keywords: CVD-ZnS; Dilatometer; SEM; XRD; IR transmission; Fractography

1. Introduction

Zinc sulphide exists in two crystallographic forms of sphalerite (cubic) and wurtzite (hexagonal) and the transformation of sphalerite phase to wurtzite phase occurs at 1020 °C [1]. The cubic form of zinc sulphide is well known as a transparent ceramic and is very widely used for IR optical engineering applications in the spectral region of 3–10 μm. Though zinc sulphide can be prepared by various processing routes, chemical vapour deposition (CVD) is commonly employed for the preparation of optical grade ZnS [2–5]. CVD, being a gas phase reaction, offers significant advantages over other methods of materials processing in view of the ease of accurately controlling the physico-chemical properties [6]. CVD reaction utilizes the chemical reaction between zinc vapor and hydrogen sulphide gas at preset temperatures and pressures to form zinc sulphide in the cubic phase [7,8]. During CVD process the grains in which the (1 0 0) plane is parallel to the substrate surface grow more rapidly and leads to the development of columnar structure. Though the CVD ZnS offers close to theoretical transmission in the range of 7–10 μm, the transmission in the visible and 3–5 μm regions is poor. Additionally, the presence of Zn–H absorption band at 6.2 μm limits its multi-spectral capability [2,10,11]. Hence, post-CVD thermal treatments are essential to improve the transmission properties in the shorter wave length region as well as to remove absorption bands [9]. Authors have reported the effect of post thermal treatments of CVD ZnS on its optical properties [12]. It was shown that post CVD pressureless heat treatments results in the elimination of Zn–H absorption band while hot isostatic pressing (HIP) at elevated temperatures has been proven to be quite effective in achieving the desired improvements in transmission in the shorter wavelength in addition to the removal of Zn–H band [12]. The temperature regime mostly reported for HIP is 950–1000 °C (around half the melting point of ZnS) and the pressure required is greater than the yield pressure of 120 MPa [13,14]. As these heat treatment regimes are close to the crystallographic transformation temperature of

* Corresponding author.
E-mail address: royjohnson@arci.res.in (R. Johnson).

0272-8842/$36.00 © 2011 Elsevier Ltd and Techna Group S.r.l. All rights reserved.
doi:10.1016/j.ceramint.2010.11.032

sphalerite to wurtzite (1020 °C), it is of interest to study the effects of this phase transformation on the microstructural, mechanical properties, fracture behaviour and optical properties of CVD derived ZnS.

2. Experimental

2.1. Sample preparation

Monolithic ZnS has been grown in a laboratory scale CVD reactor (M/s. MPA Industrie, France) by the CVD reaction between zinc (99.99%) and hydrogen sulphide (99.5%) at elevated temperatures of 650–750 °C and low pressures of around 50 mbar. The Zinc to H_2S molar ratio was adjusted close to 1.0 and a deposition rate of 80–100 μm/h was achieved by controlling the reactant fluxes. The samples were grown on graphite substrates in the form of flat plates of dimensions 50 mm × 50 mm × 5–6 mm thickness. The samples were subjected to post CVD heat treatments in a PID controlled inert gas furnace at 850 °C and 1050 °C under argon atmosphere. These samples were ground and optically polished on both sides to a final thickness of around 5 mm. The samples were designated as CVD for as CVD deposited samples, CVD-HT850 for samples heat treated at 850 °C and CVD-HT1050 for samples heat treated at 1050 °C.

2.2. Dilatometric transformation studies

CVD ZnS bars of 25 mm length × 6 mm × 6 mm cross section were ground and polished parallel on both sides to ensure close contact of the push rod and loaded in an alumina sample holder of a NETZSCH (402/C) single pushrod dilatometer. The specimens were heated from 30 to 850 and 1050 °C at a heating rate of 10 K/min under argon atmosphere and the dimensional changes were continuously recorded.

2.3. Characterization of specimens

X-ray diffraction patterns were recorded on CVD, CVD-HT850 and CVD-HT1050 samples using Bruker D8-Advanced XRD system with Cu-K_α radiation. In addition to XRD phase identification lattice parameters were also estimated for cubic and hexagonal phases. The samples were polished as per the standard metallographic procedures and micro structural characterizations were conducted using Hitachi S-4300 SE/N scanning electron microscope equipped with a field emission gun system. The specimens were also subjected to knoop hardness measurement (as per ASTM #1326 08e1) using microhardness tester (Leica, Germany) under 100 g load. The three point bend strength measurements were carried out on 40 mm × 4 mm × 3 mm thick specimens (as per ASTM # C-1161) using a UTM (Instron-4483). IR Transmission measurements were also carried out on optically polished samples of identical thicknesses using FTIR (Spectrum GX, Perkin Elmer, Singapore) in 3–10 μm spectral regions.

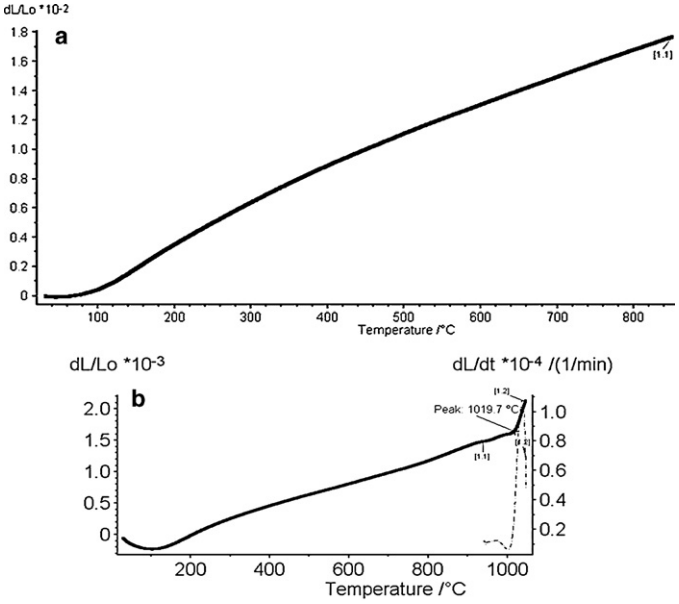

Fig. 1. Dilatometric curve showing thermal expansion with temperature (a) 30–850 °C and (b) 30–1050 °C. Note the sharp change slope at ∼1020 °C indicating the transformation.

3. Results and discussion

3.1. Crystallographic transformation

Fig. 1 presents the dilatometric plots of dL/L_0 with temperature for CVD-ZnS samples recorded in the temperature range of 30–850 and 30–1050 °C. It is evident from the plot that there exists a linear variation in the dilatometric strain when the sample is treated in the temperature range of 30–850 °C. However, on further increasing the temperature a sudden change in slope is observed at temperature close to 1020 °C indicative of the sphalerite to wurtzite transformation [1].

The XRD patterns of CVD, CVD-HT850 and CVD-HT1050 are provided in Fig. 2 CVD and CVD-HT850 samples have shown phase pure sphalerite while CVD-HT1050 specimens has shown characteristic peaks of wurtzite at 2θ values of 27° confirming the above observation of dilatometry. The CVD-HT850 sample indicated that all diffraction peaks have either disappeared or minimized in combination with an increase in reflection of (1 1 1) diffraction peaks, indicating preferential orientation. XRD peak of CVD-HT1050 at around 2θ values of 27° together with the peak at 28.6° (2θ), confirmed the coexistence of wurtzite and sphalerite phases. Lattice parameters, unit cell volumes, *c*/*a* ratio are evaluated for the specimens and are presented in Table 1. The *c*/*a* ratio of 1.633 calculated for the wurtzite phase indicates that of ideal hexagonal crystal structure.

3.2. Microstructure

Fig. 3 shows the microstructure of the CVD 650, CVD-HT850 and CVD-HT1050 specimens. The material deposited by CVD shows linear array of columnar grains, oriented parallel to the direction of coating as is evident from the cross

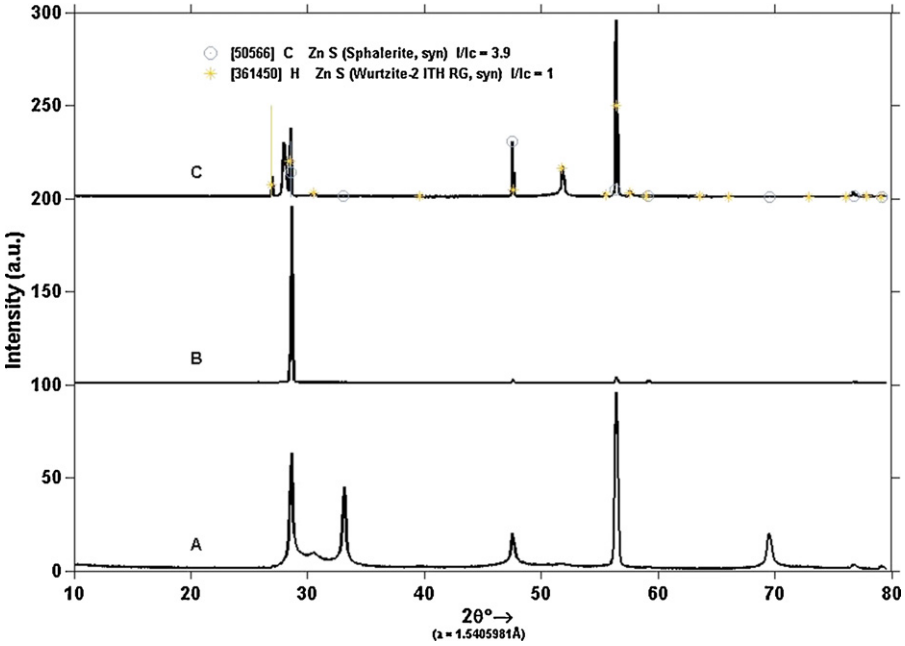

Fig. 2. XRD data of the ZnS material in the (a) CVD, (b) CVD-HT850 °C and (c) CVD-HT1050 °C process conditions.

sectional view in Fig. 3b [15]. The maximum grain sizes are found to be in the range of 5–10 μm. Most significant manifestation, of high temperature heat treatment under argon in the pressure less condition, on microstructure is the significant extent of grain growth. The average grain size is found to be in the range of 30–40 μm for CVD-HT850 samples which is further increased to ∼100 μm for CVD-HT1050 samples. This is also in combination with the transformation to wurtzite phase on increase of temperature to 1050 °C in CVD-HT1050 condition. Karakisina reported mosaic twin microstructures structures for high temperature HIP of ZnS CVD samples attributing it to the recrystallisation behaviour [13] Fang et al. also reported a similar effect where the pebble microstructure is disappeared when annealed by HIP [15,16]. The present study also indicated that similar mechanisms are operative even under pressure less annealing at temperatures of 850 and 1050 °C.

3.3. Optical properties

CVD650, CVD-HT850 and CVD-HT1050 specimens are characterized for their IR transmission properties. CVD 650 and CVD-HT850 specimens indicated similar optical properties, which is in contrast with that of the CVD-HT1050 samples. This can be attributed to the phase formation of optically anisotropic hexagonal wurtzite phase in CVD-HT1050, from the sphalerite phase with optically isotropic cubic crystallography in CVD 650 and CVD-HT850 samples (Fig. 4).

Table 1
Lattice parameters of the ZnS specimens, heat treated at different temperatures.

Condition	Crystal structure	Lattice parameter in (Å)	Lattice volume in $(Å)^3$
CVD	Cubic	$a = 5.408$	158.2
CVD-HT850 °C	Cubic	$a = 5.407$	158.1
CVD-HT1050 °C	Cubic	$a = 5.407$	158.1
	hexagonal	$a = 3.822$	79.00
		$c = 6.244$	

CVD650 samples were found to exhibit relatively high transmission levels of 65–70% in the IR wave length range of 7–10 μm and a relatively low transmission of 25–40% in the wavelength region of 3–5 μm. Additionally, the sample also exhibited 6.2 μm absorption band indicating the presence of Zn–H formed because of the reaction between zinc and hydrogen during CVD reactions. Drezner et al. [14] had reported the formation of Zn–H bonds at point defects in bulk sites or more probably in surface sites such as closed pores and grain boundaries, in CVD Zinc sulphide.

On post-CVD thermal treatment at 850 °C, CVD-HT850 indicated close to theoretical transmission of 70–75% in the 7–10 μm regions and 45–65% in the wavelength region of 3–5 μm. Additionally, the heat treatment also resulted in the elimination of Zn–H absorption band at 6.2 μm. The secondary grain growth associated with CVD-HT850 specimens resulted in homogeneity of grain sizes and their distribution, favoring the increase in IR transmission. Moreover, retention of sphalerite phase at 850 °C, prevented deterioration in transmission by virtue of its cubic crystallography [16].

Further, on heat treatment at 1050 °C, the sample CVD-HT1050 has shown a drastic decrease in transmission to <10% in the IR range of 3–5 μm and 20–45% in the 7–10 μm region. Zn–H absorption band is also absent in the spectrum. Such a significant decrease in transmission can be attributed to the formation of optically anisotropic hexagonal structure of ZnS formed due to the transformation at around 1020 °C. Liang and Rishi experimentally confirmed through their study that wurtzite phase significantly affect the IR transmission

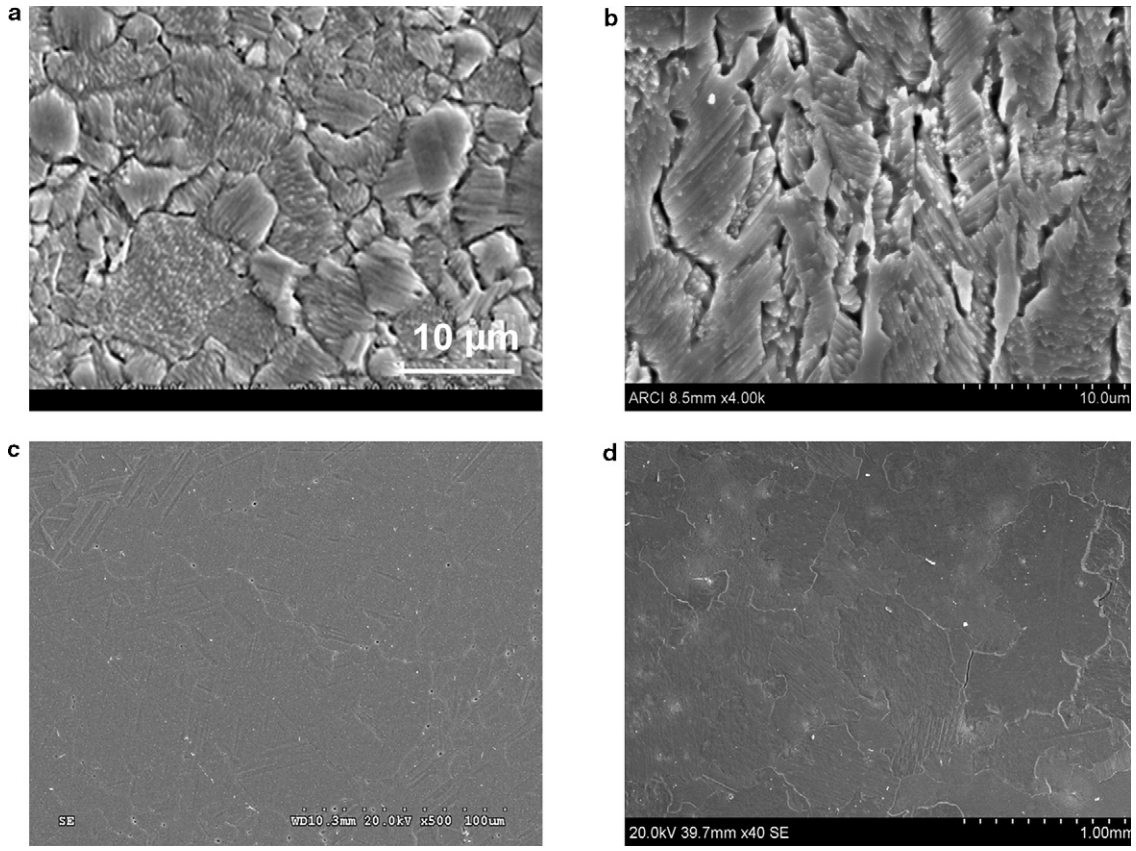

Fig. 3. SEM micrographs showing the grain size variation in the ZnS material processed in the (a) CVD surface, (b) CVD cross section, (c) CVD-HT850 °C and (d) CVD-HT1050 °C conditions.

[17,18]. It is also reported, that hexagonal crystallography exhibit birefringence effect which results in optical scatter [19]. In view of these contributing factors, the transformation to hexagonal wurtzite phase drastically affect the optical properties, especially in the shorter wave length region.

3.4. Mechanical properties

Figs. 5 and 6 show the variation in hardness and flexural strength for CVD650, CVD-HT850 and CVD-HT1050 specimens. A knoop hardness of 209 kg/mm^2, is observed for CVD650 sample which decreases to about 148 kg/mm^2 for CVD-HT850 °C and further increases to about 205 kg/mm^2 for CVD-HT1050. The flexural strength of specimens also decreased from 100 MPa in CVD650 to 60 MPa for CVD-HT850 and increased further to 76 MPa for CVD-HT1050.

The surface hardness and flexural strength is influenced by the grain size of the material and is dependent on the CVD deposition temperature and post CVD thermal treatment temperatures. The decrease in both hardness and flexural

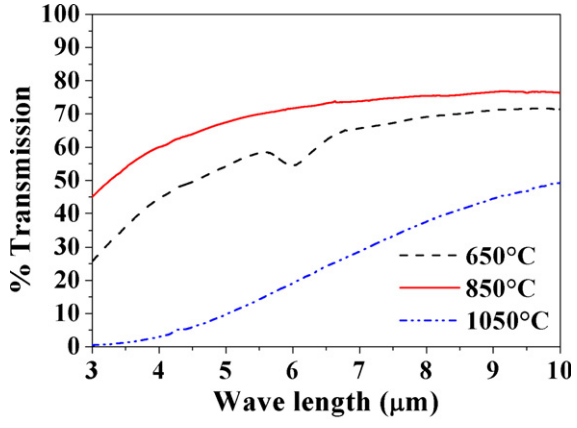

Fig. 4. Variation of optical transmission with the wave length of IR radiation.

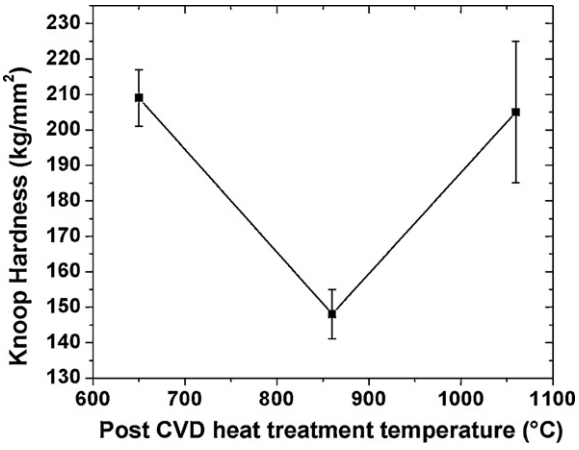

Fig. 5. Variation in the knoop hardness with process temperature.

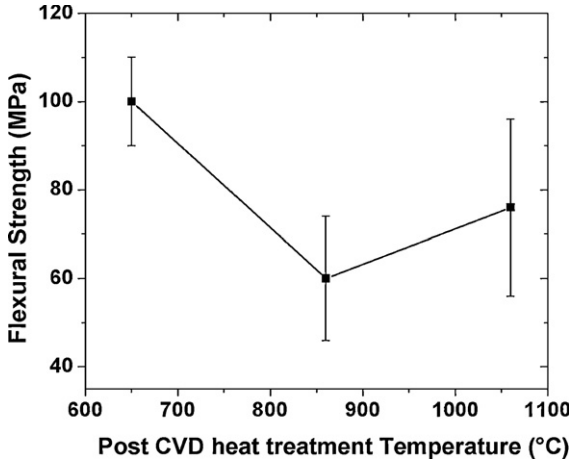

Fig. 6. Variation in the flexural strength with process temperature.

strength in CVD-HT850 can be attributed to the significant increase in grain size showing inverse relation with grain size matching with Hall–Petch relation [20,21]. Further, such grain size increase too adversely affects the mode of fracture (as will be discussed in Section 3.5) exhibiting lower flexural strength.

On the other hand, the co-existence of the sphalerite and wurtzite in the CVD-HT1050 specimen restored the mechanical properties of both hardness and flexural strength to a reasonable level. The grain size in these specimens are quite high as ~100 μm compared to the single phase field of sphalerite (5–10 μm) of CVD 650 and 30–40 μm for CVDHT-850. In order to elucidate this observation, detailed fractographic analysis was carried out and the fracture behaviour associated with the extent of low energy quasi-cleavage facet fracture was estimated in terms of percentage quasi-cleavage fracture (%QCF). In the mixed mode of fracture, transgranular shear fracture with micro dimples and QCF is possibly responsible for the restoration of flexural strength in the case of CVD-HT1050. In this material, variation in the hardness and flexural strength seems to follow similar trends. Such observations can be attributed to the uniform distribution of microstructure, especially grain and second phase particles. We are in the process of evaluating uni-axial tensile strength (all first trails have resulted in failure at the grip portion of the specimen, possible due to low tensile strength). Observed simultaneous increase in both hardness and flexural strength can be explained only after establishing a correlation between hardness, flexural strength and tensile strength which is under investigation.

3.5. Fracture behaviour

SEM fractographs obtained from the CVD650, CVD-HT850 and CVD-HT1050 specimens tested till failure under flexural

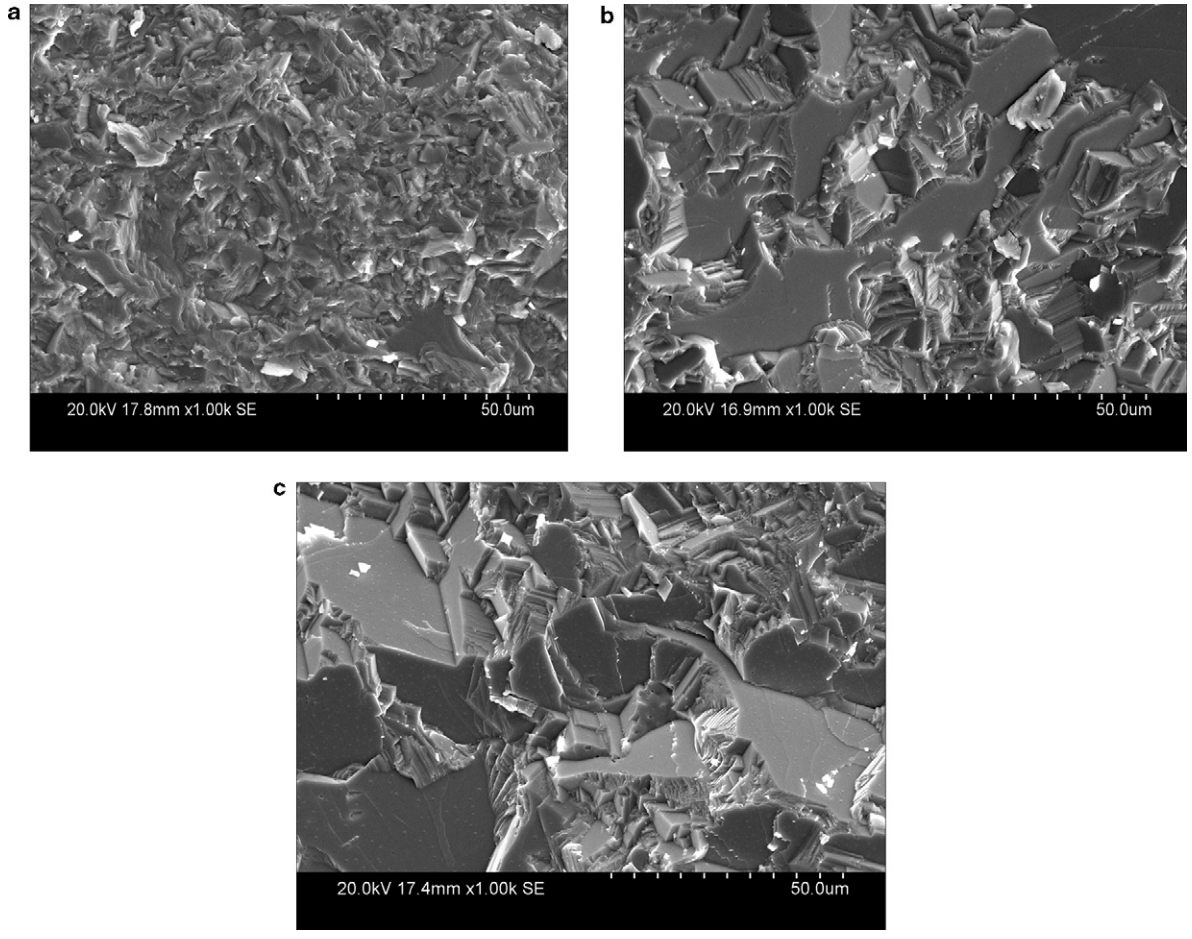

Fig. 7. SEM fractographs showing the fracture features of the ZnS material in the (a) CVD, (b) CVD-HT850 °C and (c) CVD-HT1050 °C conditions.

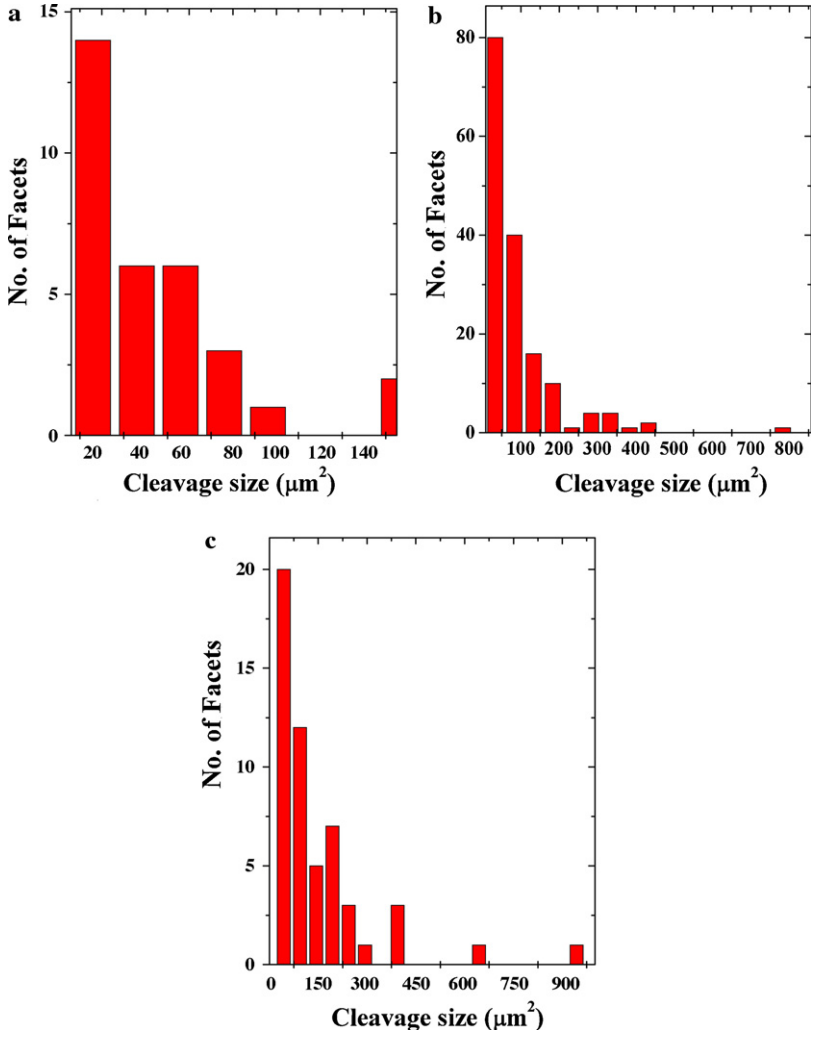

Fig. 8. Statistical variation in the cleavage facet size in (a) CVD, (b) CVD-850 °C and (c) CVD-1050 °C process conditions.

(3-point bend loading) testing are shown in Fig. 7. Planometer measurements have been performed on 10–15 fractographs taken on different locations. The technique is inherently of slightly high variation and acceptance of error bar limit of 5–10%. Though large number of fractographs at different magnifications is obtained in each of the three process conditions, for the sake of clarity only one representative fractograph for each condition, i.e., CVD (Fig. 7a), CVD-HT850 (Fig. 7b) and CVD-HT1050 (Fig. 7c) are included. These fractographs clearly show that the ZnS material in all the

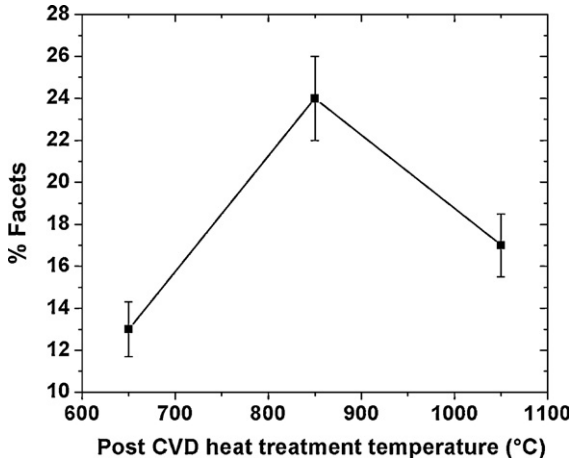

Fig. 9. Variation in % cleavage facet area with process temperature in ZnS material.

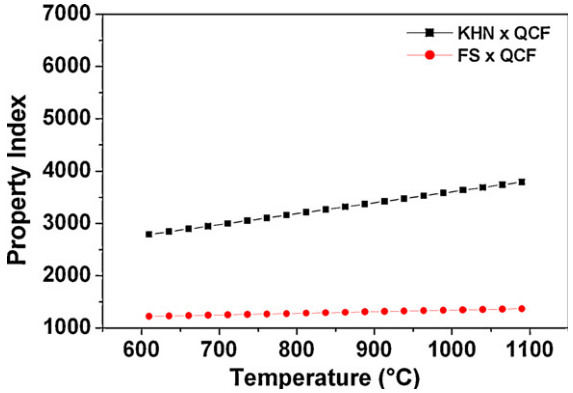

Fig. 10. Variation of property (knoop hardness and flexural strength) index with processing for ZnS ceramics.

three conditions fails by mixed fracture comprising low degree of ductile, microdimples and transgranular shear fracture, with predominant extent of low energy quasi-cleavage faceted fracture. In case of the CVD (Fig. 7a), the size of the quasi-cleavage facets are much finer. This is because of the fact that the ZnS material is of finer grain size in the range of 5–10 μm as is evident from the micrographs in Fig. 3a and b. The fracture facets under these conditions are comprised of more cleavage planes where fracture initiated needs to relocate additional facets in the neighboring grains for further crack extension. Such process needs higher fracture energy as compared to the situation where in the cleavage facets have to encounter less number of grain boundaries. In addition, the higher the energy required for the fracture process, the material would withstand fracture till higher stresses. Such high fracture stresses facilitate the formation of more number of microdimples and higher extent of transgranular shear fracture.

In CVD-HT850 with bigger grain sizes, the facets are much coarser and the extent of microdimples and transgranular shear is much lower (see Fig. 7b); thus, resulting in much lower flexural strength and fracture energy. The CVD-HT1050 material with still coarser grain sizes exhibited higher flexural strength compared to that in the CVD-HT850 condition, pointing to the possibility that the cohesive strength of the hexagonal wurtzite phase is significantly higher. This should result in net decrease in the cleavage facet area and is indeed found to be the case from the results of fractographic analysis presented below.

Detailed fractographic analysis was conducted in order to establish that the size and area fraction of the cleave facets for CVD650, CVD-HT850 and CVD-HT1050 specimens which control the mechanical properties, i.e., both knoop hardness and the flexural strength. For each of the three process conditions of CVD, CVD-HT850 and CVD-HT1050, ten representative fractographs were subjected to statistical analysis. For this purpose, the cleave facets were idealized as of rectangular cross section and the facet size (measured in terms of facet cross sectional area, % quasi-cleavage fracture, %QCF) and its number density (in terms of number of facets per unit fracture surface area) are determined. The variation of these values for the three process conditions are shown in Figs. 8 and 9. The data in Figs. 8 and 9 were employed to arrive at the property index for the knoop hardness and flexural strength, respectively as: index with processing for ZnS ceramics $(\text{property index})_{KH} = \%QCF/100 \times KHN$ and (property index) $\sigma_f = \%QCF/100 \times \sigma_f$, The property index values thus arrived at for the three process conditions are shown in Fig. 10. The data in Fig. 10 clearly shows that the property index remains almost the same for the three process conditions thus confirming the fact that the %QCF is inversely proportional to the property level, either knoop hardness or the flexural strength and indeed, is the controlling factor for the observed properties in the present material. In terms of the property variation (either KHN (knoop hardness) or flexural strength) is more than 50%, on the other hand such variation is significantly reduced when we consider the property index (of the order of ±16%). This had lead to the fact that the strength of this material is controlled by quasi cleavage fracture.

4. Conclusions

1. Both dilatometric and XRD studies confirm that the cubic sphalerite to hexagonal wurtzite transformation occurs in ZnS material at around 1020 °C.
2. Microstructural evaluation reveals that post CVD heat treatments results in secondary grain growth and significant increase in the grain size of the ZnS.
3. Increase in grain size is found to be beneficial for the IR transmission in case of the CVD-HT850 samples with sphalerite (cubic) phase, while the presence of wurtzite (hexagonal) phase reduces the IR transmission significantly for CVD-HT1050 samples.
4. Both knoop hardness and flexural strength of ZnS were found to decrease for CVD-HT850. This has been attributed to the considerable increase in the grain size.
5. Coexistence of the sphalerite and wurtzite for the CVD-HT1050 seem to restore the mechanical properties to a reasonable level despite the fact that grain size are quite high (∼100 μm) as compared to CVD-HT850 (30–40 μm) where only the single phase field of sphalerite exists.
6. Detailed quantitative fractographic analysis reveals that the mechanical properties, evaluated in the present study, scale with the extent of quasi-cleavage fracture. The higher the %QCF, the lower is either the knoop hardness or the flexural strength.

References

[1] L.A. Xue, R. Raj, Super plastic deformation of zinc sulfide near its transformation temperature (1020 °C), J. Am. Ceram. Soc. 72 (1989) 1792–1796.
[2] J.A. Savage, Infrared Optical Materials and Their Antireflection Coatings, Adam Hilger, Bristol, 1985, 95–111.
[3] J.A. Savage, K.L.A. Lewis, M. Pitt, R.H. Whitehouse, The role of CVD reactor in studies of the growth and physical properties ZnS infrared material SPIE, Adv. Opt. Mater. 505 (1984) 47–51.
[4] J.S. Goela, L.R. Taylor, Monolithic material fabrication by chemical vapor deposition, J. Mater. Sci. 23 (1988) 4331–4339.
[5] D.C. Harris, Frontiers in infrared window and dome materials, in: B.F. Andresen, M.S. Scholl (Eds.), Proc. SPIE Infrared Technology XXI, 2552, 1995.
[6] D.C. Harris, M. Boronowski, L. Henneman, L. LaCroix, C. Wilson, S. Kurzius, B. Burns, K. Kitagawa, J.S. Gembarovic, M. Goodrich, C. Staats, J.J. Mecholsky, Thermal, structural, and optical properties of Cleartran® multispectral zinc sulfide, Opt. Eng. 47 (2008) 114001–114011.
[7] F. Zhenyi, C. Yichao, H. Yongliang, Y. Yaoyuan, D. Yanping, Y. Zewu, T. Hongchang, X. Hongtao, W. Heming, CVD growth of bulk polycrystalline ZnS and its optical properties, J. Cryst. Growth 237 (2002) 1707–1710.
[8] A. Camphell, C. Haymen, Manufacturing aspects of ZnS, in: Proc. SPIE vol 09, Recent Developments in Infrared Components and Sub systems, 1988, 70–88.
[9] A.F. Shchurov, E.M. Gavrishchuk, V.B. Ikonnikov, E.V. Yashina, A.N. Sysoev, D.N. Shevarenkov, Effect of hot isostatic pressing on the elastic and optical properties of polycrystalline CVD ZnS, Inorg. Mater. 40 (2004) 336–339.
[10] S. Muskant, Optical Materials – An Introduction to Science and Application, Marcel Dekker, New York, 1985, 137.
[11] K.L. Lewis, G.S. Arthur, S.A. Banyard, Hydrogen-related defects in vapour-deposited zinc sulphide, J. Cryst. Growth 66 (1984) 125–136.
[12] P. Biswas, R.S. Kumar, P. Ramavath, V. Mahendar, G.V.N. Rao, U.S. Hareesh, R. Johnson, Effect of post CVD thermal treatments on crystal-

lographic orientation, microstructure, mechanical and transmission properties of ZnS ceramics, J. Alloys Compd. 496 (2010) 273–277.
[13] E.V. Karaksina, V.B. Ikonnikov, E.M. Gavrishchuk, Recrystallisation behaviour of ZnS during hot isostatic pressing, Inorg. Mater. 43 (2007) 452–454.
[14] Y. Drezner, S. Berger, M. Hefetz, A correlation between microstructure composition and optical transparency of CVD-ZnS, Mater. Sci. Eng. B 87 (2001) 59–65.
[15] E.V. Yashina, E.M. Gavrishchuk, V.B. Ikonnikov, Mechanisms of poly crystalline CVD ZnS densification during hot isostatic pressing, Inorg. Mater. 40 (2004) 901–904.
[16] Z. Fang, W. Pan, M. Fang, S. Shi, Morphologies and defects in CVD ZnS and Zn Se, Key Eng. Mater. 280 (2005) 537–540.
[17] V.L. Bredikhin, et al., Optical losses in polycrystalline CVD ZnS, Inorg. Mater. 45 (2009) 235–241.
[18] A.X. Liang, R. Raj, Effect of hot pressing temperature on the optical transmission of zinc sulphide, Appl. Phys. Lett. 58 (1991) 441–443.
[19] R. Apetz, M.P.B. van Bruggen, Transparent alumina: a lighting scattering model, J. Am. Ceram. Soc. 86 (2003) 480–486.
[20] C.S. Chang, J.L. He, Z.P. Lin, The grain size effect on empirically determined erosion resistance of ZnS, Wear 255 (2003) 115–120.
[21] J. McCloy, R. Korenstein, B. Zelinski, Effects of temperature, pressure, and metal promoter on the recrystallized structure and optical transmission of chemical vapor deposited zinc sulfide, J. Am. Ceram. Soc. 92 (2009) 1725–1731.